Supporting Information

Compositional Engineering of Metal-Xanthate Precursors toward $(Bi_{1-x}Sb_x)_2S_3$ ($0 \leq x \leq 0.05$) Films with Enhanced Room-Temperature Thermoelectric Performance

Zhenyu-Hu[1,2,3], Longhui-Deng[2,3], Tingjun-Wu[3], Jing Wang[4], Feiyan-Wu[4], Lie Chen[4], Qikai-Li,[5] Weishu-Liu[5], Shui-Yang Lien[6], Peng Gao[2,3*]

1. College of Chemistry, Fuzhou University, Fuzhou, Fujian, 350108, China
2. CAS Key Laboratory of Design and Assembly of Functional Nanostructures, Fujian Provincial Key Laboratory of Nanomaterials, Fujian Institute of Research on the Structure of Matter, Chinese Academy of Sciences, 155 Yangqiao Road West, Fuzhou 350002, China
3. Xiamen Institute of Rare Earth Materials, Xiamen Key Laboratory of Rare Earth Photoelectric Functional Materials, Chinese Academy of Sciences, Xiamen 361021, China
4. College of Chemistry, Nanchang University, 999 Xuefu Avenue, Nanchang 330031, China.
5. Department of Materials Science and Engineering, Southern University of Science and Technology, Shenzhen 518055, China.
6. School of Opto-electronic and Communication Engineering, Xiamen University of Technology, Xiamen 361024, China

[*]Corresponding author. E-mail address: peng.gao@fjirsm.ac.cn

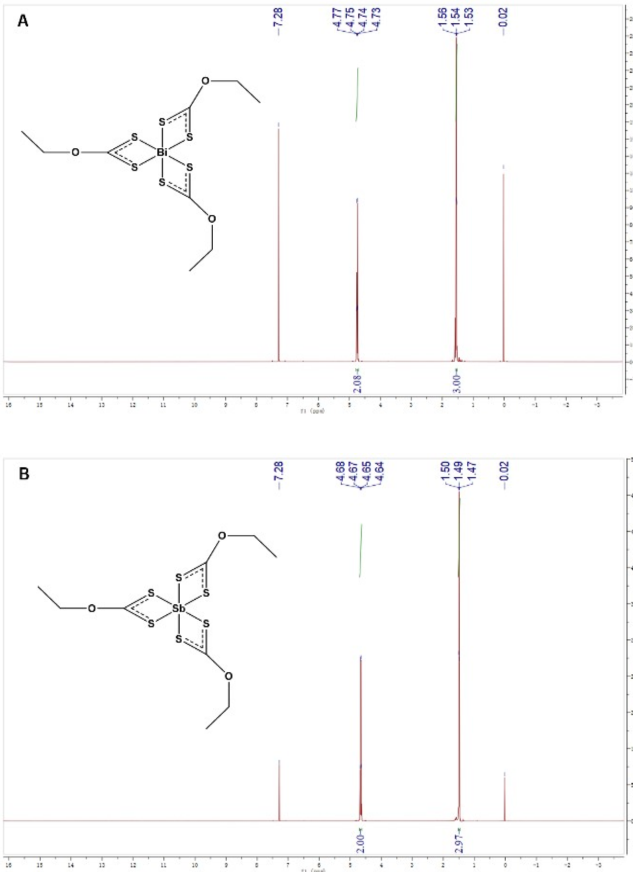

Figure. S1 A and B are the ^{1}H NMR spectrum of $Bi(S_2COEt)_3$ and $Sb(S_2COEt)_3$ in $CDCl_3$.

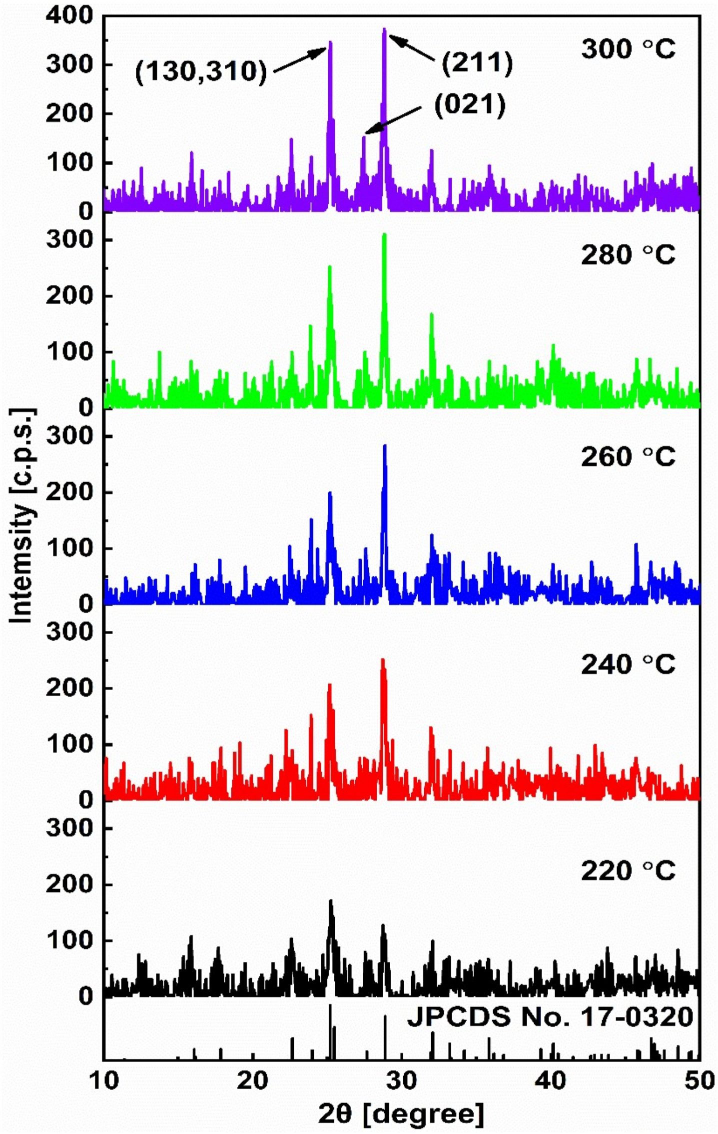

Figure. S2 XRD pattern of Bi_2S_3 thin films annealing at 220 °C, 240 °C, 260 °C, 280 °C, 300 °C.

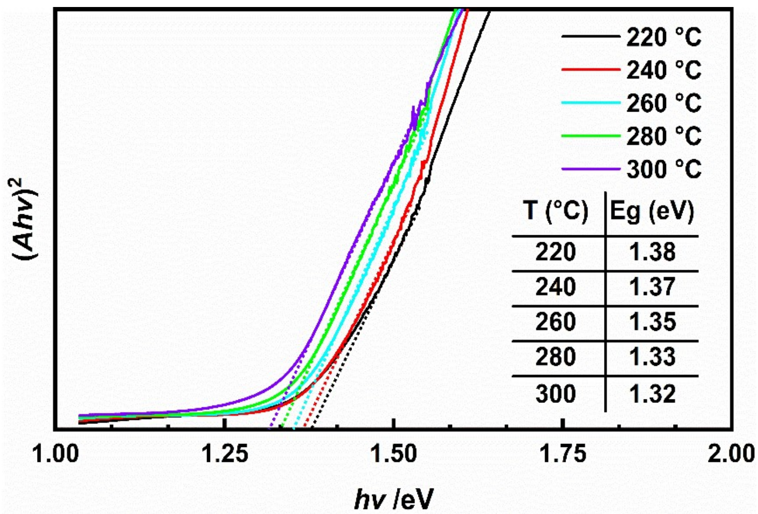

Figure. S3 Temperature dependence of Tauc plot spectrums for Bi_2S_3 thin films.

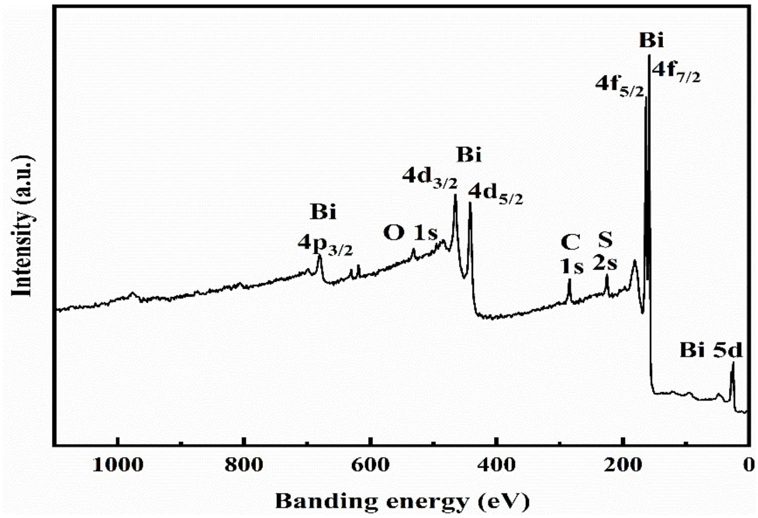

Figure. S4 XPS survey spectrum of a pristine Bi_2S_3 film annealed at 300 °C.

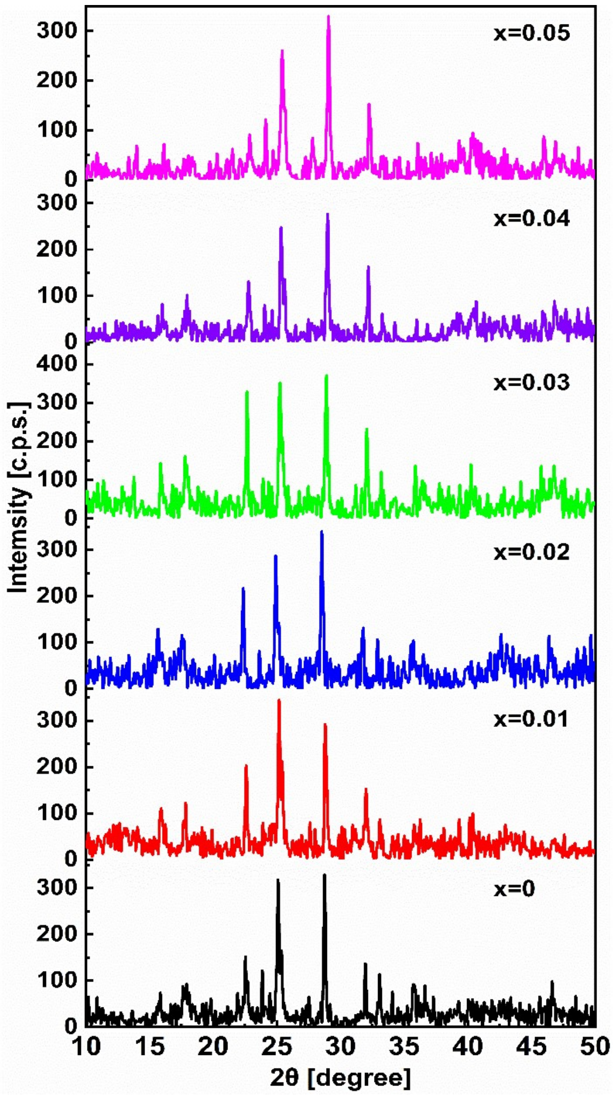

Figure. S5 XRD pattern of $(Bi_{1-x}Sb_x)_2S_3$ ($0 \leq x \leq 0.05$) films annealed at 300 °C

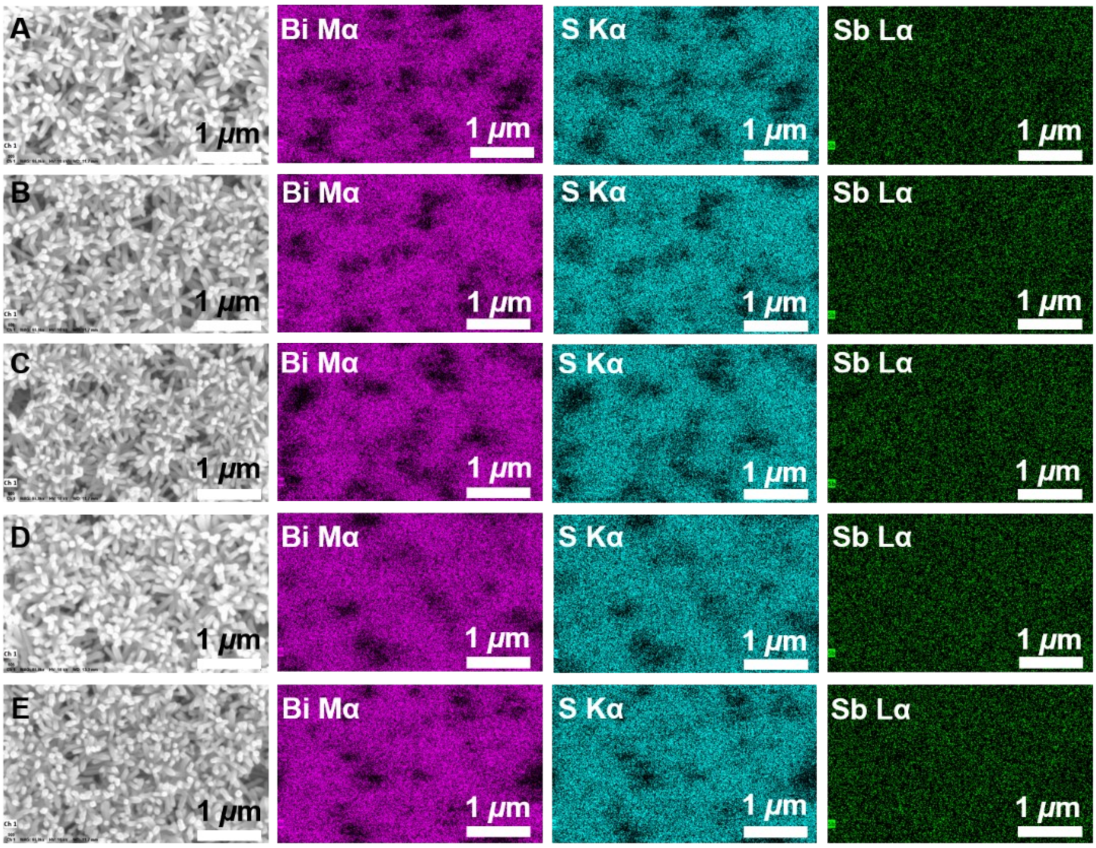

Figure. S6 Energy Dispersive Spectrometer (EDX) elemental mapping (10 kV) of Bi Mα, Sb Lα and S Kα for $(Bi_{1-x}Sb_x)_2S_3$ samples. (A) x = 0.01, (B) x =0.02, (C) x = 0.03, (D) x = 0.04 and (E) x=0.05 mole fractions of antimony.

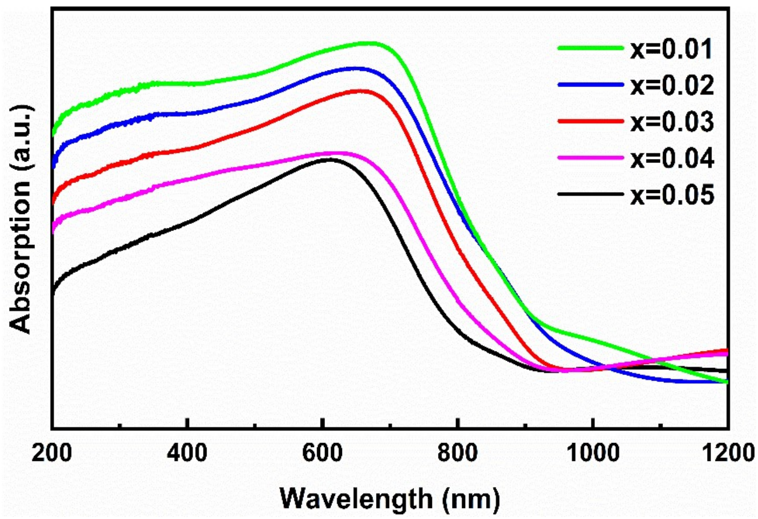

Figure. S7 Absorption spectra of $(Bi_{1-x}Sb_x)_2S_3$ ($0.01 \leq x \leq 0.05$).

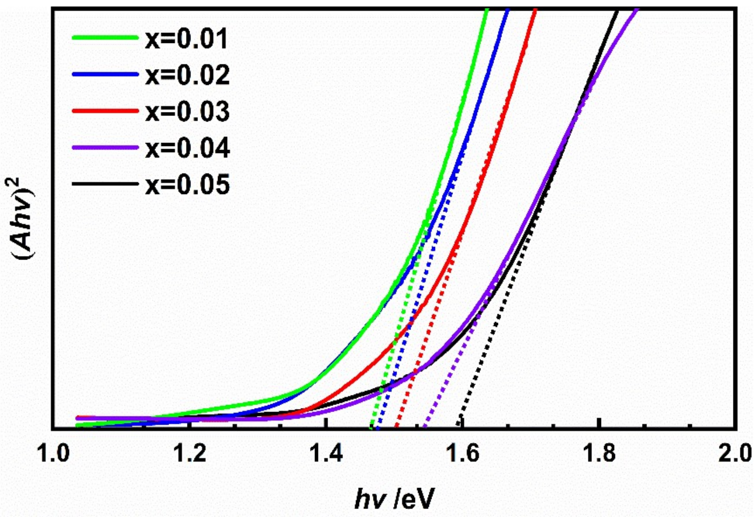

Figure. S8 Tauc plot for the $(Bi_{1-x}Sb_x)_2S_3$ (0.01≤ x ≤0.05)

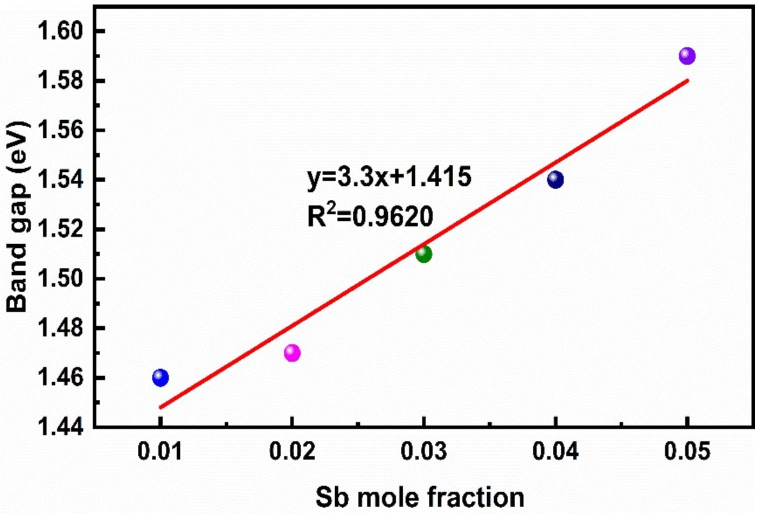

Fig. S9 Variation of the band gap for $(Bi_{1-x}Sb_x)_2S_3$ (0.01≤x≤0.05) samples as a function of mole fraction (x) of Sb.

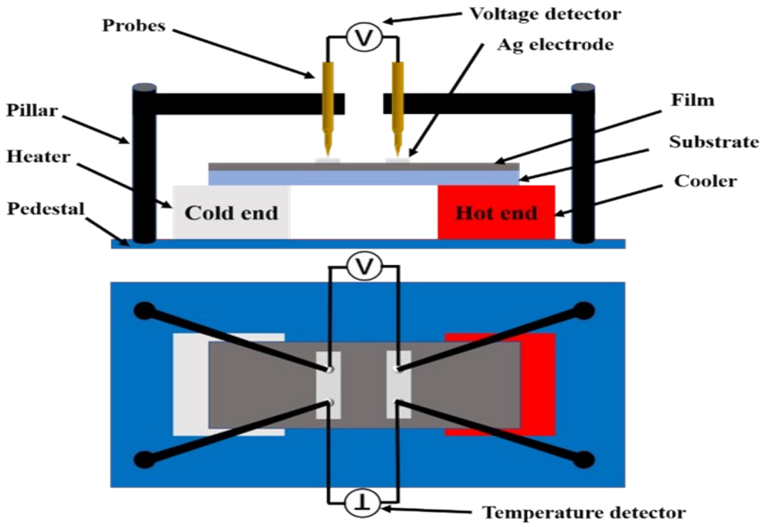

Figure. S10 Schematic of home-made for Seebeck coefficient measurement; above is the positive view, below is top view.

Table S1 The thickness of Bi_2S_3 film measured by surface stylus profiler.

Concentration (mol L^{-1})	Thickness (nm)
0.15	117.4
0.2	160.6
0.25	196.9
0.3	260.9

Table S2 The lattice parameter of *a*-, *b*- and *c* axis and crystalline analysis about $(Bi_{1-x}Sb_x)_2S_3$ ($0 \le x \le 0.05$) solid solution series.

		Sb mole fraction (x)					
		0	0.01	0.02	0.03	0.04	0.05
Lattice axis (Å)	*a*	11.1500	11.1533	11.1566	11.1589	11.1612	11.1639
	b	11.3489	11.3566	11.3697	11.3770	11.3849	11.3931
	c	3.9724	3.9626	3.9567	3.9483	3.9390	3.9317
Crystalline analysis	*V* (nm^3)	502.664	501.917	501.896	501.256	500.525	500.079
	D (nm)	96.8762	78.9706	64.4241	45.9183	38.4402	36.3471
	δ ($\times 10^{14}$ nm^{-2})	1.0655	1.6035	2.4094	4.7427	6.7675	7.5694
	N ($\times 10^{16}$ nm^{-2})	1.5983	2.4053	3.6141	7.1141	10.1513	11.3541

#Note: XRD calculation of $(Bi_{1-x}Sb_x)_2S_3$ ($0 \le x \le 0.05$) films

(1). The volume of the cell was estimated using the equation

$$V = abc$$

(2). The crystallite size was decided using Scherrer equation

$$D = \frac{K\gamma}{B\cos\theta}$$

K=0.89 is Scherrer's constant; *B* is the FWHM of the diffraction peak of the measured sample; θ is Bragg diffraction angle; γ is wavelength of X-ray, generally 1.5406 Å.

(3) Dislocation density of thin films can be determined using the equation [1]

$$\delta = 1/D^2$$

(4) Number of crystallites/unit area can be obtained using relationship [2]

$$N = t/D^3$$

t is the thickness of thin films.

Table. S3 Annealing temperature dependences of the carrier transport properties of Bi_2S_3 thin films, 5 samples were collected for each variable

Annealing temperature (℃)	Sample (#)	n ($\times10^{19}$cm^{-3})	Mean/ variance	μ (cm^2 V^{-1} s^{-1})	Mean/ variance	$\sigma_h{}^a$ (S cm^{-1})	Mean/ variance
220	#1	2.215	2.291/ 0.128	1.204	1.184 /0.069	4.273	4.340/ 0.131
	#2	2.193		1.235		4.339	
	#3	2.510		1.069		4.297	
	#4	2.301		1.238		4.564	
	#5	2.238		1.179		4.228	
240	#1	1.455	1.463/ 0.045	2.907	2.900/ 0.108	6.777	6.798/ 0.285
	#2	1.503		2.867		6.904	
	#3	1.402		3.045		6.840	
	#4	1.442		2.746		6.344	
	#5	1.513		2.939		7.124	
260	#1	0.807	0.885/ 0.083	7.445	7.297/ 0.142	9.626	10.353/ 0.940
	#2	1.010		7.195		11.643	
	#3	0.912		7.328		10.708	
	#4	0.813		7.110		9.261	
	#5	0.887		7.409		10.529	
280	#1	0.781	0.779 /0.023	11.271	11.4/ 0.094	14.103	14.227/ 0.405
	#2	0.785		11.391		14.326	
	#3	0.753		11.399		13.752	
	#4	0.813		11.403		14.853	
	#5	0.763		11.536		14.102	
300	#1	0.198	0.196/ 0.010	45.268	45.576/ 0.546	14.360	14.305/ 0.522
	#2	0.207		45.019		14.930	
	#3	0.189		45.951		13.914	
	#4	0.202		45.308		14.663	
	#5	0.184		46.336		13.659	

[a] The electrical conductivity (σ_h) calculated by $\sigma = ne\mu$.

[b] The electrical conductivity (σ_f) measured with a four-point probe technique.

Table. S4 Concentration of precursor dependences of the carrier transport properties of Bi_2S_3 thin films, 5 samples are collected for each variable.

Concentration (mol L^{-1})	Sample (#)	n ($\times10^{19}cm^{-3}$)	Mean/ variance	μ ($cm^2\,V^{-1}\,s^{-1}$)	Mean/ variance	$\sigma_h{}^a$ ($S\,cm^{-1}$)	Mean/ variance
0.15	#1	0.197	0.1918/ 0.006	8.837	8.839/ 0.506	2.789	2.712/ 0.080
	#2	0.195		8.490		2.653	
	#3	0.189		8.755		2.651	
	#4	0.197		8.424		2.659	
	#5	0.181		9.691		2.810	
0.2	#1	0.443	0.428/ 0.061	13.90	14.239/ 0.873	9.868	9.708/ 0.967
	#2	0.332		15.298		8.137	
	#3	0.431		14.970		10.337	
	#4	0.434		13.772		9.576	
	#5	0.502		13.207		10.622	
0.25	#1	1.036	0.958/ 0.077	5.041	5.075/ 0.10	8.367	7.793/ 0.671
	#2	0.847		4.940		6.703	
	#3	0.929		5.154		7.671	
	#4	0.951		5.205		7.930	
	#5	1.028		5.037		8.296	
0.3	#1	1.265	1.328/ 0.068	3.299	3.260/ 0.189	6.686	6.951/ 0.403
	#2	1.372		3.488		7.667	
	#3	1.308		3.254		6.819	
	#4	1.425		2.970		6.780	
	#5	1.273		3.337		6.806	

[a] The electrical conductivity (σ_h) calculated by $\sigma = ne\mu$.

[b] The electrical conductivity (σ_f) measured with a four-point probe technique.

Table S5 Sb mole fraction dependences of the carrier transport properties of Bi_2S_3 thin films, 5 samples are collected for each variable.

Sb mole fraction	Sample (#)	n ($\times10^{19}$cm^{-3})	Mean/ variance	μ (cm^2 V^{-1} s^{-1})	Mean/ variance	σ_h[a] (S cm^{-1})	Mean/ variance
0.01	#1	0.250	0.247/ 0.019	6.531	6.461/ 0.291	2.616	2.566/ 0.298
	#2	0.216		6.088		2.107	
	#3	0.247		6.664		2.637	
	#4	0.270		6.785		2.935	
	#5	0.254		6.241		2.540	
0.02	#1	0.279	0.271/ 0.044	9.188	9.56/ 0.633	4.107	4.130/ 0.455
	#2	0.326		8.844		4.619	
	#3	0.204		10.366		3.388	
	#4	0.265		10.067		4.274	
	#5	0.285		9.341		4.265	
0.03	#1	0.378	0.380/ 0.017	14.450	14.409/ 0.474	8.751	8.776/ 0.118
	#2	0.384		14.390		8.853	
	#3	0.362		14.989		8.693	
	#4	0.371		14.545		8.646	
	#5	0.408		13.671		8.937	
0.04	#1	0.541	0.514/ 0.031	3.260	3.364/ 0.260	2.826	2.764/ 0.173
	#2	0.478		3.805		2.914	
	#3	0.502		3.120		2.510	
	#4	0.496		3.356		2.667	
	#5	0.553		3.280		2.906	
0.05	#1	1.851	1.831/ 0.105	0.714	0.745/ 0.039	2.117	2.187/ 0.189
	#2	1.690		0.779		2.108	
	#3	1.773		0.716		2.034	
	#4	1.967		0.798		2.516	
	#5	1.875		0.720		2.163	

[a] The electrical conductivity (σ_h) calculated by $\sigma = ne\mu$.

[b] The electrical conductivity (σ_f) measured with a four-point probe technique.

Table S6 Electrical resistivity(σ), Seebeck coefficient, and power factor for the Bi_2S_3 films in present work and other typical TE films at room temperature.

Method	Sample	σ ($S\cdot cm^{-1}$)	Seebeck ($\mu V\cdot K^{-1}$)	PF ($\mu W\cdot m^{-1}\cdot K^2$)	Ref.
Spin-coating and annealing	Bi_2S_3 films	10.32	-388.33	155.63	**This work**
Melting and Spark plasma sintering (SPS)	Bi_2S_3 bulk	4	-352	49.56	3
Nanocomposite pellet	Bi_2S_3@Bi bulk	39.65	-97.38	37.66	4
SPS	Bi_2S_3@Bi bulk	38.89	~-150	~87.50	5
Melting and SPS	$(Bi_{0.2}Sb_{0.8})_2S_3$ bulk	2.52×10^{-3}	~-450	~0.05	6
Electron Beam and Spin-coating	Bi_2S_3 films	6.0	-21.41	0.28	7
Wet chemical synthesis	Bi_2S_3 films	5×10^{-3}	~-650	0.02	8
Chemical Bath Deposition	Bi_2S_3 films	50	-755	2850	9
Melting–SPS	Sb_2Se_3 whisker	~1	~-200	~2	10
SPS	$Bi_{1.995}Cu_{0.005}S_3$ bulk	14.41	~-275	~108.97	11

References

1 P. A. Chate and V. D. Bhabad, *Int. J. Mod. Trends Sci. Technol.*, 2016, **2**, 6–11.

2 M. Dhanam, R. R. Prabhu and P. K. Manoj, *Mater. Chem. Phys.*, 2008, **107**, 289–296.

3 K. Biswas, L.-D. Zhao and M. G. Kanatzidis, *Adv. Energy Mater.*, 2012, **2**, 634–638.

4 Tarachand, G. S. Okram, B. K. De, S. Dam, S. Hussain, V. Sathe, U. Deshpande, A. Lakhani and Y. K. Kuo, *ACS Appl. Mater. Interfaces*, 2020, **12**, 37248–37257.

5 Z. H. Ge, P. Qin, D. He, X. Chong, D. Feng, Y. H. Ji, J. Feng and J. He, *ACS Appl. Mater. Interfaces*, 2017, **9**, 4828–4834.

6 Y. Kawamoto and H. Iwasaki, *J. Electron. Mater.*, 2014, **43**, 1475–1479.

7 J. Recatala-Gomez, H. K. Ng, P. Kumar, A. Suwardi, M. Zheng, M. Asbahi, S. Tripathy, I. Nandhakumar, M. S. M. Saifullah and K. Hippalgaonkar, *ACS Appl. Mater. Interfaces*, 2020, **12**, 33647–33655.

8 N. P. Klochko, V. R. Kopach, I. I. Tyukhov, G. S. Khrypunov, V. E. Korsun, V. O. Nikitin, V. M. Lyubov, M. V. Kirichenko, O. N. Otchenashko, D. O. Zhadan, M. O. Maslak and A. L. Khrypunova, *Sol. Energy*, 2017, **157**, 657–666.

9 S.-C. Liufu, L.-D. Chen, Q. Yao and C.-F. Wang, *Appl. Phys. Lett.*, 2007, **90**, 112106.

10 H. J. Wu, P. C. Lee, F. Y. Chiu, S. W. Chen and Y. Y. Chen, *J. Mater. Chem. C*, 2015, **3**, 10488–10493.

11 Z. H. Ge, B. P. Zhang, Y. Liu and J. F. Li, *Phys. Chem. Chem. Phys.*, 2012, **14**, 4475–4481.